HHS Public Access

Author manuscript

*Brain Res Bull*. Author manuscript; available in PMC 2019 September 29.

Published in final edited form as:

*Brain Res Bull*. 2018 September ; 142: 88–95. doi:10.1016/j.brainresbull.2018.06.015.

# Long-term effects of curcumin in the non-human primate brain

**Bang-Bon Koo**[a,*,1], **Samantha Calderazzo**[a,1], **Bethany G.E. Bowley**[a], **Alekha Kolli**[b], **Mark B. Moss**[a,b,c], **Douglas L. Rosene**[a,c], **Tara L. Moore**[a,b]

[a]Department of Anatomy and Neurobiology, School of Medicine, Boston University, Boston, MA, USA

[b]BA/MD Program, Boston University, Boston, MA, USA

[c]Department of Neurology, School of Medicine, Boston University, Boston, MA, USA

## Abstract

Curcumin has recently been shown to be a potential treatment for slowing or ameloriating cognitive decline during aging in our nonhuman primate model of normal aging. In these same monkeys, we studied for the first time the neurological impacts of long-term curcumin treatments using longitudinal magnetic resonance imaging (MRI). Sixteen rhesus monkeys received curcumin or a vehicle control for 14–18 months. We applied a combination of structural and diffusion MRI to determine whether the curcumin resulted in structural or functional changes in focal regions of the brain. The longitudinal imaging revealed decreased microscale diffusivity (mD) measurements mainly in the hippocampus and basal forebrain structures of curcumin treated animals. Changes in generalized fractional anisotropy (GFA) and grey matter density (GMd) measurements indicated an increased grey matter density in cortical ROIs with improved white matter integrity in limbic, cerebellar, and brain stem regions. These findings suggest that noticeable changes in the neuronal environment could be induced from long-term curcumin treatments. Results may provide a neurological basis on the recent findings demonstrating improved spatial working memory and motor function in nonhuman primates.

### Keywords

Curcumin; Brain; MRI; Diffusion; Cognition; Memory; Aging; Restricted diffusion; Logitudinal; Rhesus monkey

## 1. Introduction

Studies of both humans and non-human primates have demonstrated that age-related cognitive decline begins as early as the fifth decade and typically the earliest changes occurring in the domain of executive function which is mediated by the prefrontal cortex

*Corresponding author at: Department of Anatomy and Neurobiology, School of Medicine, Boston University, Boston, MA 02118, USA. bbkoo@bu.edu (B.-B. Koo).

[1]1st Authors.

Conflict of interest

The authors have no conflict of interest to declare.

(Cahn-Weiner et al., 2000; Fristoe et al., 1997; Lai et al., 1995; Moore et al., 2003, 2006; Hara et al., 2012; León et al., 2016). Interestingly, there is also significant evidence for age-related changes in PFC white matter and myelin (Bowley et al., 2010; Drag and Bieliauskas, 2010; Guttmann et al., 1998; Makris et al., 2007; Peters and Sethares, 2002) and it is thought that inflammation may underlie this white matter pathology and myelin breakdown and therefore anti-inflammatory comounds are potential interventions (Cornejo and von Bernhardi, 2016; Xie et al., 2013).

Curcumin, a naturally occurring compound of the ginger family and the primary active ingredient in the spice turmeric, is a powerful anti-inflammatory and anti-oxidant and therefore may slow or delay progression of age-related changes in cognitive functions (Cox et al., 2015; Aggarwal and Harikumar, 2009). In fact, epidemiological studies revealed a potential link between curcumin consumption and a lower prevalence of cognitive decline in older adults (Ng et al., 2006) and studies with animal models also support that curcumin could help prevent deficits in memory and cognitive function during the aging process (Dong et al., 2012; Nam et al., 2014).

Using our non-human primate model of normal aging, we have administered oral doses of curcumin to middle-aged rhesus monkeys in order to determine whether the monkeys would experience improvement in cognition. The monkeys receiving commercially available Longvida® Optimized curcumin that was manufactured and supplied by Verdure Sciences (Noblesville, IN).revealed a delayed pattern of decline in their spatial working memory and motor function (Moore et al., 2017, 2018).

The enhancement of cognitive performance in our monkeys could be due to increases in neurogenesis (Dong et al., 2012), neurotransmitter modulation (Kumar et al., 2010) or suppressing glia-induced inflammation (Yuan et al., 2017). Moreover, increases in inflammatory microglia and subsequent myelin damage in these animals have been shown to correlate with such impairments (Peters and Kemper, 2012; Shobin et al., 2017). Likewise, inflammation can lead to myelin damage with age, which may slow conduction velocities in important white matter tracts (di Penta et al., 2013; Cragg and Thomas, 1961; Smith and Koles, 1970; Babbs and Shi, 2013). However, curcumin has been shown to up regulate the regeneration of myelin sheaths after injury (Yu et al., 2016). Specifically, curcumin has significant effects in cortical and sub-cortical regions including the medial prefrontal cortex (Noorafshan et al., 2017), the hippocampus (Liu et al., 2014; Zheng et al., 2017), the amygdala (Zhang et al., 2012) and the spinal cord (Yuan et al., 2017). In monkeys the hippocampus plays a significant role in spatial and recognition memory, while more contributions to the latter is expected (Beason-Held et al., 1999). There are also emerging evidences for the complementary roles between the hippocampus and cortical structures in spatial memory functioning (Wang and Morris, 2010; Koo et al., 2013). Hence, differential effects of curcumin are thereby expected across the cortical and subcortical structures in rhesus macaques. However, the precise actions of curcumin in the brain remain unclear.

Recently, magnetic resonance imaging (MRI) has been successfully applied to assess the effect of curcumin in vivo. Structural MRI (T2 and T2* imaging) in rat model of spinal cord injury (Yuan et al., 2017) and stroke (Miao et al., 2016) revealed successful differentiation of

the curcumin treatment effects. Although those studies limited the use of MRI to qualitative assessment on the treatment effect, structural MRI has been also proven to offer a key imaging marker for assessing changes in the brain in other studies (Alexander et al., 2008; Wisco et al., 2008; Koo et al., 2012). Diffusion MRI is another imaging solution which could tackle changes in the brain in micro-scale. The tissue water diffusion information can be potentially sensitive to many factors including axons, dendrites, myelinated fibers or non-neuronal components (Gulani et al., 2001; Anwander et al., 2010; McNab et al., 2013). Therefore, variations in the tissue environment might be expressed in a mixture of diverse diffusion patterns, such as microscopic (i.e., hindered) and fast diffusivities. Each of these variant patterns can be captured in specific ranges of diffusion encodings in MRI. Recent studies have shown that micro-scale diffusion can be a sensitive measurement to the micro-structural changes in the brain (Jespersen et al., 2010), such as the astroglial plasticity induced by learning task (Blumenfeld-Katzir et al., 2011) or mild traumatic brain injury (Singh et al., 2016). Since previous findings on curcumin pinpointed subneuronal changes (Dong et al., 2012; Yuan et al., 2017), diffusion MRI is expected to provide in-depth figure on monitoring treatment effects.

This current study sought to investigate the effects of long-term curcumin treatment on the rhesus macaque brain. It is, to our knowledge, the first in-vivo imaging assessments of the long-term curcumin treatments on rhesus monkeys, a developed model for normal aging. All monkeys in the treatment group received curcumin treatment for 14–18 months. We then applied structural and diffusion MRI to determine whether the observed effects of curcumin can be localized to a specific area of the brain.

## 2. Methods

### 2.1. Subjects

Seventeen, behaviorally naive, middle-aged adult (11–21 years of age), male and female rhesus monkeys (Macaca mulatta) were recruited in this study. All of the monkeys were obtained from a national primate research facility or private vendor and had known birth dates and complete health records. Before entering the study, monkeys received medical examinations that included serum chemistry, hematology, urine analysis, and fecal analysis. Although all monkeys received same imaging and cognitive assessments, one female monkey was excluded for the analysis due to the reconstruction error on the follow up scan. Age- and gender information of 16 monkeys are listed in the Table 1.

The monkeys were individually housed in colony rooms where they were in constant auditory and visual range of other monkeys in the Animal Science Center (ASC) of Boston University Medical Campus. This facility is fully AAALAC approved and animal maintenance and research were conducted in accordance with the guidelines of the National Institutes of Health and the Institute of Laboratory Animal Resources Guide for the Care and Use of Laboratory Animals. All procedures were approved by the Institutional Animal Care and Use Committee of the Boston University Medical Campus. Diet consisted of Purina Monkey Chow (Purina Mills Inc., St. Louis, MO) supplemented by fruit with feeding taking place once per day, immediately following behavioral testing. All monkeys were fed 12–20 biscuits per day based on their weight. During testing, small pieces of fruit or candy were

used as rewards. Water was available continuously. The monkeys were housed under a 12-h light/dark cycle with cycle changes occurring in a graded fashion over the course of an hour. Following a quarantine period, acclimation to the colony room and baseline testing, monkeys were randomly assigned to either a control or curcumin treatment group.

Prior to beginning daily control or curcumin administration, all monkeys were initially familiarized with behavioral testing in a Wisconsin General Testing Apparatus (WGTA) where they were trained to displace a single gray plaque on a wooden testing board to obtain a reward. Monkeys then were administered the delayed non-matching to Sample task (DNMS), a benchmark recognition memory task that assesses the ability of subjects to identify a novel stimulus from a familiar stimulus following a 10-s delay interval.

The day after reaching criterion on the initial acquisition of the DNMS basic task, the monkeys were randomly assigned to either the curcumin treatment or control groups and began receiving their daily dose of 500 mg of dietary curcumin treatment or control for 2 weeks. This dosage of curcumin was chosen based on review of several clinical trials (https://clinicaltrials.gov/ct2/results?cond=&term=curcumin&cntry=&state=&city=&dist=).

The curcumin used in this study was Longvida® Optimized curcumin that was manufactured and supplied by Verdure Sciences (Noblesville, IN). Their formulation is optimized natural curcumin that was lipidized for enhanced bioavailability (https://vs-corp.com/longvida/). The control was dextrin and tartrazine (to match the color of active curcumin). The curcumin and control were mixed with approximately 120–150 ml of yogurt or Prima-BurgerTM (BioServ, Flemington, NJ) and frozen. A single treatment was given to each monkey following cognitive testing each day. Treatments were also administered on the weekends and holidays. A technician observed the monkey to confirm the treatment was eaten completely. If a monkey would not eat the treatment (e.g., discarding or dropping it into the waste pan of their cage), a second treatment was given. Monkeys ate the treatments (both the control and curcumin) on more than 98% of the study days.

At the end of the 2-week period of initial dosing with curcumin or control, monkeys began the first of three rounds of cognitive testing, while continuing daily doses of curcumin or control. At the end of each round of testing, the monkeys were not tested for 8 weeks, but continued to receive their daily dose of curcumin or control. At the end of the 8-week period, they began the next round of testing, while continuing to receive daily curcumin or control. During each round of cognitive testing (approximately 6–8 months in duration), monkeys completed the following cognitive tests: Re-acquisition of DNMS delays (2-min delays), and Delayed Recognition Span Task (Spatial, DRSTsp) and our task of fine motor function, the Hand Dexterity Task (HDT) (See Moore et al., 2017, 2018 for details).

Briefly, the findings from the cognitive testing were that monkeys receiving daily oral doses of curcumin evidenced a greater improvement in performance on the DRSTsp task, as compared with monkeys that received a control substance (Table 1). In contrast, there was no difference between the curcumin and control group on DNMS with a 120-s delay. In addition, monkeys receiving curcumin demonstrated no changes on the fine motor task

(−0.58 ± 1.6%) in round 2 of testing compared to round 1 while control group showed declined pattern (−9 ± 3.8%).

### 2.2. Imaging

Magnetic resonance imaging was completed prior to entering the study and at the end of each round of testing. All experiments were performed on a whole body 3 T MRI Philips scanner (Philips Medical Systems, Best, the Netherlands). For all scans, monkeys were sedated with Ketamine (10 mg/kg), an IV line was then placed in the saphenous vein and a continuous Propofol IV infusion (0.3–0.4 mg/kg/min) was started. Monkeys were then intubated and all critical vital signs were monitored through the scan time.

The radio-frequency (RF) coil used for this experiment was the 6-channel synergy receive-only head coil, while RF transmission was done through the quadrature body coil. The six channels in the head coil were combined in quadrature mode. Monkeys were secured in an MRI-compatible stereotactic head-holder designed to fit within the RF coil used for the experiment.

Structural MRI image was acquired using a T1-weighted 3D-turbo field echo (TFE) sequence that was fully optimized to provide high signal to noise ratio (SNR) and high gray-white matter contrast at high resolution with following parameters: TR/TE 7 ms/3 ms, flip angle 8, NEX 6, intershot delay 2800 ms, TFE factor 200, voxel size: 0.6/0.6/0.6 mm, sagittal plane acquisition. Diffusion Spectrum Imaging (DSI) was collected based on the diffusion spectrum imaging scheme (Wedeen et al., 2008). DSI parameters were as follows: voxel size of 2 mm isocubic, FOV 5 160 mm, TR/TE 3590/50, number of directions 128, multiple high b-values, half Q-space acquisition, NSA 5 1, flip angle 5 90, sense factor of 2 in the AP direction, with a total scan time of approximately in 35 min.

### 2.3. Image processing

To provide a unified analysis framework, we applied the same anatomical definitions to both T1 and DSI analysis. Processing was done based on the pipeline, which applied in our previous study (Koo et al., 2013). However, there were some modification on the pipeline. In this study, we applied INIA19 rhesus monkey template for segmentation and automatic labeling of local region of interests (ROI) in the subject brain. INIA19 template was registered to the subject structural MRI based on linear transformation. Template's tissue prior information was also transformed to the structural MRI using the same parameters obtained in the previous step and used for the basis on tissue segmentation (Zhang et al., 2001). Gray matter tissue segment was used as gray matter density (GMd) for the analysis. Nonlinear transformation was then applied to the template to register it into the structural MRI (Greve and Fischl, 2009). Template's predefined ROIs were then non-linearly transformed to the structural MRI to extract regional average GMd in each ROIs in the subject space.

DSI was registered to the structural MRI following the motion and eddy current distortion correction (Jenkinson et al., 2012). Subject ROIs in the structural MRI space were then inverse transformed to the DSI to define regions in the diffusion MRI. Q-space imaging method (Yeh et al., 2010) were used for the reconstruction of diffusion parameters. Three

dimensional probability information on the diffusion displacement was calculated in each voxel in the brain scans and then formed the spin distribution function. Micro-scale diffusivity (mD) was modeled for partial diffusion encoding length based on the weighted sum of partial spin distributions below upper bound of the diffusion displacement (Yeh et al., 2016). In this study, we applied same upper bound used in our previous study (Koo et al., 2018) for calculating the micro-scale diffusivity maps. We also calculated generalized fractional anisotropy (GFA) based on the spin distribution in q-space reconstruction. GFA has been used for quantifying micro-structural integrity (similar to fractional anisotropy in diffusion tensor imaging) for q-space diffusion imaging. Mean value of mD or GFA were calculated based on the subject ROIs in diffusion space.

### 2.4. Statistical analysis

Percent change in the follow-up from the baseline imaging was calculated based on the following formula: (followup – baseline)/baseline × 100. Mean values of each ROIs in each group were calculated and assessed for differences between the groups. Independent sample *t*-statistics was used to test the group differences. Age was controlled. A permutation approach (Anderson and Robinson, 2001) using 10,000 iterations was used to calculate statistical inferences for all statistical analyses.

## 3. Results

### 3.1. Micro-scale diffusivity (mD)

The curcumin treated group showed decreased mD patterns in the follow-up observations. Statistically significant change patterns were confirmed mainly in sub-cortical ROIs. ROIs revealing statistically significant differences are shown in Fig. 1 and Table 2. In the left hippocampal ROIs (#428, #438 and #74), a 12 to 15 percent decrease in mD from baseline measurements were shown in the curcumin treated group while control groups showed increased mD in those ROIs. Group differences in mD percent change values were shown in the dendate gyrus (#438). Adjacent to the left hippocampus, the left entorhinal ROI (#166) and the lateral geniculate nucleus (#130) revealed significant decreases in mD in post-treatment compared to the baseline scans in the curcumin treated group. Two ROIs in the basal forebrain structures (#454, #968) also showed a decrease in mD in post-treatment scans. Statistical values on these ROIs are listed in Table 2.

Decreased mD in the follow-up scans were also confirmed in ROIs in the brain stem (#608, #621). The right middle cerebeller peduncle (#608) showed 18.38% decrease in mD for the curcumin group ($t = -2.31$, corrected $p < 0.05$). Also, the right side of the pontine nuclei showed about 13 percent decrease in post scan mD measurement whereas the control group revealed 25 percent increase in average. In those regions highlighted from mD mapping, no significant changing patterns were observed in other imaging measures (Fig. 1A,C,D,F). In the cortex, only 2 ROIs (#215, #556) revealed significant group differences in percent change on mD. The left fronto-orbital gyrus (#556) and the right superior temporal gyrus were highlighted from the mD mapping.

### 3.2. Generalized FA (GFA) and gray matter density (GMd)

GFA and GMd mapping also highlighted ROIs in the sub-cortical and the brain stem (Fig. 2 and Table 2). However, there were additional ROIs shown in the cerebellum, prefrontal and inferior temporal ROIs. All ROIs with significant group differences in GFA did not overlap with the ROIs shown in mD assessments.

In GFA, the curcumin treated group revealed significant group differences in percent change measure of the right hippocampal ROIs, #930 and #668. However, the patterns were not consistent across the ROIs. Curcumin treated group revealed increased patterns in the former (#930) while decreased patterns shown in the latter ROI (#668). Control group showed an opposite pattern in those ROIs to the curcumin group (see Table 2, GFA section). In the sub-cortical region, left basal forebrain nucleus (#466) showed increased pattern while control group showed opposite pattern. GFA measure also highlighted ROIs in the brain stem (#358, #361). The curcumin treated group showed increased GFA in the brain stem and both ROIs were in the opposite side of the brain stem to those shown in the mD mapping (#608, #621). In cortical and cerebellar gray matter ROIs (#213 and #229), the curcumin group showed decreased GFA percent change pattern. Moreover, the left middle frontal gyrus revealed highest group difference pattern ($T = -2.87$, correct $p < 0.01$) among other GFA percent change measures.

In GMd assessments, the left entorhinal area (#166) was highlighted for significant group differences in percent change value. Similar to the mD assessments, the left enthorhinal area in curcumin treated group showed decreased patterns. Other 2 hippocampal ROIs also revealed decreased pattern in GMd (#425 and #432). Control groups showed all increased pattern in those ROIs. Highest group differences in GMd were shown in the right lateral amygdala nucleus (#691) and the biventer lobule of cerebellum (#755). All cortical ROIs showed increased patterns in GMd in the follow up scans of curcumin group (#509 and #507).

## 4. Discussions

In this study, 10 mid-aged rhesus monkeys received curcumin treatments and 6 age and gender matched control monkeys were recruited for comparison. Multi-modal in-vivo imaging including structural and diffusion MRI was used to investigate potential longitudinal effects of curcumin in the brain over a two year period. Structural MRI was used to assess changes in the local gray matter structures while the diffusion MRI was applied to capture micro-structural information in brain regions. From the diffusion MRI, mD mapping was used to detect sub-neuronal or micro-glial changes. GMd was used to measure macroscopic tissue changes, while GFA was used to assess generalized diffusivity patterns in the brain. Considering the faster aging process in rhesus monkeys compared with humans, 14–18 months of curcumin treatments applied in this study could be considered as up to 4.5 years of treatments in humans. To our knowledge, this is the first attempt to investigate effects of curcumin on the brain in non-human primate model of normal aging.

Here, we have shown that noticeable changes in the neuronal environment could be induced from the long-term curcumin treatment. Among all imaging indices, mD revealed a

consistent decrease in patterns across ROIs with the highest changing rate compared to other imaging measures. The hippocampus (#438, #428) and the basal forebrain structures (#454, #968, #130) were highlighted in mD with the highest level of significance in group comparison, while there were additional ROIs covering cortical (#215, #556) and brain stem (#608, #621). Additionally, GFA measurements revealed decreased patterns in the prefrontal (#213) and cerebellar gray matter (#229), whereas increased patterns were found in sub-cortical and brain stem ROIs. We also confirmed increased GMd in cortical gray matter ROIs (#509, #507).

### 4.1. Anti-inflammatory effects of curcumin

In normal aging, primates have shown a reduction in cognitive abilities associated with myelin damage and white matter loss (Peters and Kemper, 2012). Although the cause of this pathology has yet to be fully determined, recent evidence suggests that inflammatory and phagocytic microglia may be involved (Shobin et al., 2017). Particularly, chronic inflammation accumulating with age can induce microglia to become hypertrophic and release cytokines, which may lead to surrounding tissue damage and inhibition of myelin repair (Karperian et al., 2013; von Bernhardi et al., 2015; Neumann et al., 2009; Lampron et al., 2015). Moreover, pathophysiological levels of cytokines, such as tumor necrosis factor-alpha (TNFa) and interleukin-1, have been shown to be detrimental to synaptic plasticity and neurogenesis (Bellinger et al., 1993; Curran and O'Connor, 2001; Gibertini et al., 1995; Goshen et al., 2008). However, curcumin has been shown to have potent anti-inflammatory effects due to its activity on the nuclear factor kappa B (NFkB) pathway. When phosphorylated by inhibitor of kappa B (IkB) kinases, NFkB translocates to the nucleus and triggers the transcription of pro-inflammatory cytokines, chemokines, and adhesion molecules (Olivera et al., 2012; Giuliani et al., 2001). Yet, curcumin can bind to peroxisome proliferator-activated receptor gamma (PPAR-y) to reduce the activity of IkB kinases and subsequently inhibit the downstream release of cytokines (Jacob et al., 2007; Siddiqui et al., 2006; Forman et al., 1996). Overall, curcumin's anti-inflammatory effects have been shown in small animals models to prevent demyelination (Yu et al., 2016), microglia response (Guo et al., 2013), and dendritic loss (Noorafshan et al., 2017). Therefore, we propose that curcumin treated monkeys may express increased synaptic organization, reduced hypertrophy of glia, and improved myelin maintenance.

### 4.2. Subtle changes of neuroinflammation as measured by mD

In our previous study of neuro-toxicant induced neuroinflammation, we illustrated that mD can be sensitive to subtle changes in the brain without the requirement of severe damage to the brain tissue (Koo et al., 2018). Specifically, higher mD was found to correlate with several pro-inflammatory cytokines, such as up-regulation in TNFa and interleukin-6 following intoxication. These pro-inflammatory markers can be released from neurons or microglia in states of inflammation, which result in changes in synaptic densities and connections (Kondo et al., 2011). Moreover, cytokines can influence microglia morphology and antigen processing (McManus et al., 1998; Tomimoto et al., 2000), which results in hypertrophic extensions and enlarged somas (Karperian et al., 2013). Therefore, we postulate that enhanced mD values are the result of increased micro-scale changes in morphology, such as arborization of dendrites or glial processes. Hence, decreased mD

patterns in the curcumin groups in this study could likely be the result of reduced inflammatory signaling and consequent changes in the brain. Recent postmortem studies also confirm curcumin treatment suppresses astrocyte-induced inflammation followed by changes in immune markers (Yuan et al., 2017). Likewise, treatment of curcumin has been shown to suppress microglial hypertrophy (Guo et al., 2013). Therefore, regions with a decreased mD in curcumin treated animals, particularly the hippocampus and basal forebrain, may indicate a reduction in glial response and inflammation. On the other hand, up-regulated patterns in mD shown in the control group (Table 2, % change in mD in the controls) may be indicative of the normal cognitive aging process as postmortem studies of rhesus monkeys confirm an increase in inflammatory microglial with aging and cognitive decline (Sloane et al., 1999; Shobin et al., 2017). Although significant microglial changes have been found mostly in the white matter (Hart et al., 2012), we did not find any statistically significant up-regulation of mD in the white matter or even in the gray matter from the control group. This could be due to the age of the animals as they are just reaching the threshold of old age.

### 4.3. Cellular organization and myelination assessed by GMd

From the multimodal imaging, we have confirmed that the curcumin treatment may have a potential impact on the cortical structures. However, changes in those imaging measures were shown in selected regions, indicating that the effect of curcumin in cortical regions may not be as significant as the pattern shown in the sub-cortical regions. Upregulated GMd, or grey matter density, in the curcumin treated monkeys in their inferior temporal (#509) and occipital regions (#507) suggest a reduction in cerebral atrophy, which could be the result of enhanced synaptic connections (Olivera et al., 2012; Giuliani et al., 2001; Bellinger et al., 1993; Curran and O'Connor, 2001; Gibertini et al., 1995; Goshen et al., 2008). Observed pattern in GMd is consistent with a previous study that found prevention of atrophic changes, such as dendrite shrinkage and spine number, in cortical areas following curcumin treatment (Noorafshan et al., 2017). Opposed to the cerebral ROIs, down-regulated GMd was confirmed in both sub-cortical and cerebellar ROIs of the curcumin group, which may reflect changes in the adjacent white matter areas (Salat et al., 2009). This result follows another study where curcumin treatment enhanced MBP expression and prevented further demyelination and oligodendrocyte apoptosis after compressed spinal cord injury (Yu et al., 2016). As shown in a previous study, such enhancement of myelination in adjacent white matter may increase T1 intensity around the ROI border and lower gray matter density measures (Koo et al., 2012). Therefore, we propose regions with lower GMd in the sub-cortical and cerebellar regions may reflect higher levels of myelin in connecting white matter regions, while increased GMd in the cortex indicates a reduction in dendritic atrophy.

### 4.4. Gray matter complexity and white matter integrity measured by GFA

In GFA mapping, the left middle frontal gyrus ROI (#213) in the curcumin group revealed significant pattern differences against the controls. In previous studies, it has been shown that the impact of aging in area 46 (overlaps to #213), is likely due to loss of dendritic arborization or synaptic integrity (reviews for Peters and Kemper, 2012), which can decrease complexity in the medium and enhance either radial or tangential diffusion components (Johnson et al., 2014; Zhuo et al., 2012). If this is the case, then lowered GFA in the frontal

cortex of curcumin treated animals can be postulated as an increased complexity due to intactness of subneuronal components. On the other hand, a protective role of curcumin in the brain stem or spinal cord has been empirically shown in recent studies (Bondan et al., 2017; Yuan et al., 2017). Effects include preventing demyelination or axonal degeneration, which can cause more structured diffusivity in the tissue medium and increase measures of white matter integrity. Hence, increase of GFA in brain stem ROIs may reflect enhanced myelination and axonal connection. Moreover, considering its role on motor function, increased myelination in either brain stem or cerebellar ROIs could provide a neurological basis of preventing degenerations of fine motor function in the middle-aged rhesus monkey following curcumin treatment (Moore et al., 2018).

### 4.5. Changes in hippocampal diffusivity may reflect improvements in spatial working memory

As shown in our previous paper, we have confirmed improvements in spatial working memory in aging non-human primates treated with curcumin (Moore et al., 2018). The hippocampus plays a significant role in spatial and recognition memory (Beason-Held et al., 1999; Wang and Morris, 2010; Koo et al., 2013), and in this study we show curcumin treated animals had significant difference in hippocampal ROIs compared to controls. Specifically, differences were shown in left hippocampal ROIs via mD and GMd, whereas 2 right hippocampal ROIs were picked up by GFA. Both mD and GMd revealed a decrease after the curcumin treatments, which could reflect reduced glia hypertrophy and increased myelination (Salat et al., 2009; Koo et al., 2018). This is consistent with recent post-mortem studies on small animal models where treatment with curcumin demonstrated changes in microglia morphology, cytokine release, and synaptic pruning (Zheng et al., 2017; Liu et al., 2014; Dong et al., 2012; Kim et al., 2008; Guo et al., 2013; Yuan et al., 2017). However, GFA measurements in the hippocampus showed either up- or down-regulated patterns. As we discussed earlier, cellular level investigation is needed to fully determine which factors produce such differences. Yet, these measurements could indicate increased synaptic density or enhanced myelination (Johnson et al., 2014; Zhuo et al., 2012), which may accompany enhancements in cognitive functions. For example, mice with enhanced hippocampal myelination performed better on the Morris water maze spatial task (Lu et al., 2016). Taken together, present findings in the hippocampus may explain previously observed cognitive enhancements in these animals and indicate replicable benefits of curcumin in non-human primates. However, further validation with in-vivo assessments is required for having a complete figure on this topic.

## 5. Conclusions

Overall, we hypothesize that curcumin’s ability to dampen inflammatory responses may increase synaptic connections and myelin maintenance. Multimodal MRI helps establish the morphological basis for how curcumin acts to improve cognition and motor skills in an aging primate model. Specifically, changes in hippocampal, brain stem, and cerebellar regions may reflect enhanced myelination in adjacent white matter, which could explain improvements in both spatial and motor tasks. Moreover, changes in frontal, inferior temporal, and occipital cortices could represent increased synaptic density and organization

that could further contribute to cognitive tasks. However, many factors can influence imaging and since diffusion MRI does not employ exogenous contrast agents to label the potential neural features, determining what exactly effects local diffusivity in different regions of the brain needs to be further confirmed with ex-vivo analysis. Although further histological validation is needed for a better understanding, the results confirm that long-term curcumin administration may have a potential impact on the brain in subneuronal components.

## Acknowledgements

Dr. Koo and Samantha Calderazzo contributed equally to this work. This study was supported by the National Institutes of Health—National Institute of AgingR01-AG043478 and R01-AG043640.

## References

Aggarwal BB, Harikumar KB, 2009 Potential therapeutic effects of curcumin, the anti-inflammatory agent, against neurodegenerative, cardiovascular, pulmonary, metabolic, autoimmune and neoplastic diseases. Int. J. Biochem Cell Biol 41 (1), 40–59. [PubMed: 18662800]

Alexander GE, Chen K, Aschenbrenner M, Merkley TL, Santerre-Lemmon LE, Shamy JL, Skaggs WE, Buonocore MH, Rapp PR, Barnes CA, 2008 Age-related regional network of magnetic resonance imaging gray matter in the rhesus macaque. J. Neurosci 28 (11), 2710–2718. [PubMed: 18337400]

Anderson MJ, Robinson J, 2001 Permutation tests for linear models. Aust. N. Z. J. Stat 43, 75–88.

Anwander A, Pampel A, Knosche TR, 2010 In vivo measurement of cortical anisotropy by diffusion-weighted imaging correlates with cortex type. Proc. Int. Soc. Magn. Reson. Med 18, 109.

Babbs CF, Shi R, 2013 Subtle paranodal injury slows impulse conduction in a mathematical model of myelinated axons. PLoS One 8 (7), e67767. [PubMed: 23844090]

Beason-Held LL, Rosene DL, Killiany RJ, Moss MB, 1999 Hippocampal formation lesions produce memory impairment in the rhesus monkey. Hippocampus 9 (5), 562–574. [PubMed: 10560927]

Bellinger FP, Madamba S, Siggins GR, 1993 Interleukin 1 beta inhibits synaptic strength and long-term potentiation in the rat CA1 hippocampus. Brain Res 628 (1–2), 227–234. [PubMed: 8313151]

Blumenfeld-Katzir T, Pasternak O, Dagan M, Assaf Y, 2011 Diffusion MRI of structural brain plasticity inducedby a learning and memory task. PLoS One 6 (6), e20678. [PubMed: 21701690]

Bondan E, Cardoso C, Martins MF, 2017 Curcumin decreases astrocytic reaction after gliotoxic injury in the rat brainstem. Arg. Neuropsiquiatr 75 (8), 546–552.

Bowley MP, Cabral H, Rosene DL, Peters A, 2010 Age changes in myelinated nerve fibers of the cingulate bundle and corpus callosum in the rhesus monkey. J. Comp. Neurol 518 (15), 3046–3064. [PubMed: 20533359]

Cahn-Weiner DA, Malloy PF, Boyle PA, Marran M, Salloway S, 2000 Prediction of functional status from neuropsychological tests in community-dwelling elderly individuals. Clin. Neuropsychol 14 (2), 187–195. [PubMed: 10916193]

Cornejo F, von Bernhardi R, 2016 Age-dependent changes in the activation and regulation of microglia. Adv. Exp. Med. Biol 949, 205–226. [PubMed: 27714691]

Cox KH, Pipingas A, Scholey AB, 2015 Investigation of the effects of solid lipid curcumin on cognition and mood in a healthy older population. J. Psychopharmacol 29 (5), 642–651. [PubMed: 25277322]

Cragg BG, Thomas PK, 1961 Changes in conduction velocity and fibre size proximal to peripheral nerve lesions. J. Phyisol 157, 315–327.

Curran B, O'Connor JJ, 2001 The pro-inflammatory cytokine interleukin-18 impairs long-term potentiation and NMDA receptor-mediated transmission in the rat hippocampus in vitro. Neuroscience 108 (1), 83–90. [PubMed: 11738133]

di Penta A, Moreno B, Reix S, Fernandez-Diez B, Villanueva M, Errea O, et al., 2013 Oxidative stress and proinflammatory cytokines contribute to demyelination and axonal damage in a cerebellar culture model of neuroinflammation. PLoS One 8 (2), e54722. [PubMed: 23431360]

Dong S, Zeng Q, Mitchell ES, Xiu J, Duan Y, Li C, Tiwari JK, Hu Y, Cao X, Zhao Z, 2012 Curcumin enhances neurogenesis and cognition in aged rats: implications for transcriptional interactions related to growth and synaptic plasticity. PLoS One 7 (2), e31211. [PubMed: 22359574]

Drag LL, Bieliauskas LA, 2010 Contemporary review 2009: cognitive aging. J. Geriatr. Psychiatry Neurol 23 (2), 75–93. [PubMed: 20101069]

Forman BM, Chen J, Evans RM, 1996 The peroxisome proliferator-activated receptors: ligands and activators. Ann. N. Y. Acad. Sci 804 (1), 266–275. [PubMed: 8993549]

Fristoe NM, Salthouse TA, Woodard JL, 1997 Examination of age-related deficits on the Wisconsin card sorting test. Neuropsychology 11 (3), 428–436. [PubMed: 9223147]

Gibertini M, Newton C, Friedman H, Klein TW, 1995 Spatial learning impairment in mice infected with Legionella pneumophila or administered exogenous interleukin-1-beta. Brain Behav. Immun 9 (2), 113–128. [PubMed: 7549035]

Giuliani C, Napolitano G, Bucci I, Montani V, Monaco F, 2001 Nf-kB transcription factor: role in the pathogenesis of inflammatory, autoimmune, and neoplastic diseases and therapy implications. Clin. Ther 152 (4), 249–253.

Goshen I, Kreisel T, Ben-Menachem-Zidon O, Licht T, Weidenfeld J, Ben-Hur T, Yirmiya R, 2008 Brain interleukin-1 mediates chronic stress-induced depression in mice via adrenocortical activation and hippocampal neurogenesis suppression. Mol. Psychiatry 13 (7), 717–728. [PubMed: 17700577]

Greve DN, Fischl B, 2009 Accurate and robust brain image alignment using boundary-based registration. Neuroimage 48 (1), 63–72. [PubMed: 19573611]

Gulani V, Webb AG, Duncan ID, Lauterbur PC, 2001 Apparent diffusion tensor measurements in myelindeficient rat spinal cords. Magn. Reson. Med 45 (2), 191–195. [PubMed: 11180424]

Guo L, Xing Y, Pan R, Jiang M, Gong Z, Lin L, Dong J, 2013 Curcumin protects microglia and primary rat cortical neurons against HIV-1 gp120-mediated inflammation and apoptosis. PLoS One 8 (8), e70565. [PubMed: 23936448]

Guttmann CR, Jolesz FA, Kikinis R, Killiany RJ, Moss MB, Sandor T, Albert MS, 1998 White matter changes with normal aging. Neurology 50 (4), 972–978. [PubMed: 9566381]

Hara Y, Rapp PR, Morrison JH, 2012 Neuronal and morphological bases of cognitive decline in aged rhesus monkeys. Age (Dordr) 34 (5), 1051–1073. [PubMed: 21710198]

Hart AD, Wyttenbach A, Hugh Perry V, Teeling JL, 2012 Age related changes in microglial phenotype vary between CNS regions: grey versus white matter differences. Brain Behav. Immun 26 (5), 754–765. [PubMed: 22155499]

Jacob A, Rongqian W, Mian Z, Wang P, 2007 Mechanism of the anti-inflammatory effect of curcumin: PPAR-γ activation. PPAR Res 2007, 89369. [PubMed: 18274631]

Jenkinson M, Beckmann CF, Behrens TE, Woolrich MW, Smith SM, 2012 FSL. Neuroimage 62 (2), 782–790. [PubMed: 21979382]

Jespersen SN, Bjarkam CR, Nyengaard JR, Chakravarty MM, Hansen B,Vosegaard T, et al., 2010 Neurite density from magnetic resonance diffusion measurements at ultrahigh field: comparison with light microscopy and electron microscopy. NeuroImage 49 (1), 205–216. [PubMed: 19732836]

Johnson GA, Calabrese E, Little PB, Hedlund L, Qi Y, Badea A, 2014 Quantitative mapping of trimethyltin injury in the rat brain using magnetic resonance histology. Neurotoxicology 42, 12–23. [PubMed: 24631313]

Karperian A, Ahammer H, Jelinek HF, 2013 Quantitating the subtleties of microglial morphology with fractal analysis. Front. Cell. Neurosci 7, 3 10.3389/fncel.2013.00003. [PubMed: 23386810]

Kim SJ, Son TG, Park HR, Park M, Kim MS, et al., 2008 Curcumin stimulates proliferation of embryonic neural progenitor cells and neurogenesis in the adult hippocampus. J. Biol. Chem 283 (21), 14497–14505. [PubMed: 18362141]

Kondo S, Kohsaka S, Okabe S, 2011 Long-term changes of spine dynamics and microglia after transient peripheral immune response triggered by LPS in vivo. Mol. Brain 4 (June (27)). 10.1186/1756-6606-4-27.

Koo BB, Schettler SP, Murray DE, Lee JM, Killiany RJ, Rosene DL, et al., 2012 Age-related effects on cortical thickness patterns of the Rhesus monkey brain. Neurobiol. Aging 33 (1) 200.e23–31.

Koo BB, Oblak AL, Zhao Y, Farris CW, Bowley B, Rosene DL, Killiany RJ, 2013 Hippocampal network connections account for differences in memory performance in the middle-aged rhesus monkey. Hippocampus 23 (12), 1179–1188. [PubMed: 23780752]

Koo BB, Michalovicz LT, Calderazzo S, Kelly KA, Sullivan K, Killiany RJ, O'Callaghan JP, 2018 Corticosterone potentiates DFP-induced neuroinflammation and affects high-order diffusion imaging in a rat model of Gulf War Illness. Brain Behav. Immun 67, 42–46. [PubMed: 28782715]

Kumar TP, Antony S, Gireesh G, George N, Paulose CS, 2010 Curcumin modulates dopaminergic receptor, CREB and phospholipase C gene expression in the cerebral cortex and cerebellum of streptozotocin induced diabetic rats. J. Biomed. Sci 17, 43. [PubMed: 20513244]

Lai ZC, Moss MB, Killiany RJ, Rosene DL, Herndon JG, 1995 Executive system dysfunction in the aged monkey: spatial and object reversal learning. Neurobiol. Aging 16 (6), 947–954. [PubMed: 8622786]

Lampron A, Larochelle A, Laflamme N, Prefontaine P, Plante MM, Sanchez MG, Yonh VW, Stys PK, Tremblay ME, Rivest S, 2015 Inefficient clearance of myelin debris by microglia impairs remyelinating processes. J. Exp. Med 212 (April (4)), 481–495. 10.1084/jem.20141656. [PubMed: 25779633]

León I, Tascón L, Cimadevilla JM, 2016 Age and gender-related differences in a spatial memory task in humans. Behav. Brain Res 306, 8–12. [PubMed: 26965569]

Liu D, Wang Z, Gao Z, Xie K, Zhang Q, Jiang H, Pang Q, 2014 Effects of curcumin on learning and memory deficits, BDNF, and ERK protein expression in rats exposed to chronic unpredictable stress. Behav. Brain Res 271, 116–121. [PubMed: 24914461]

Lu W, Yang S, Zhang L, Chen L, Chao FL, Luo YM, et al., 2016 Decreased myelinated fibers in the hippocampal dentate gyrus of the Tg2576 mouse model of Alzheimer's disease. Curr. Alzheimer Res 13 (9), 1040–1047. [PubMed: 26971933]

Makris N, Papadimitriou GM, van der Kouwe A, Kennedy DN, Hodge SM, Dale AM, Rosene DL, 2007 Frontal connections and cognitive changes in normal aging rhesus monkeys: a DTI study. Neurobiol. Aging 28 (10), 1556–1567. [PubMed: 16962214]

McManus CM, Brosnan CF, Berman JW, 1998 Cytokine induction of MIP-1 alpha and MIP-1 beta in human fetal microglia. J. Immunol 160 (February (3)), 1449–1455. [PubMed: 9570566]

McNab JA, Polimeni JR, Wang R, Augustinack JC, Fujimoto K, Stevens A, Janssens T, Farivar R, Folkerth RD, Vanduffel W, Wald LL, 2013 Surface based analysis of diffusion orientation for identifying architectonic domains in the in vivo human cortex. NeuroImage 69, 87–100. [PubMed: 23247190]

Miao Y, Zhao S, Gao Y, Wang R, Wu Q, Wu H, Luo T, 2016 Curcumin pretreatment attenuates inflammation and mitochondrial dysfunction in experimental stroke: the possible role of Sirt1 signaling. Brain Res. Bull 121, 9–15. [PubMed: 26639783]

Moore TL, Killiany RJ, Herndon JG, Rosene DL, Moss MB, 2003 Impairment in abstraction and set shifting in aged rhesus monkeys. Neurobiol. Aging 24 (1), 125–134. [PubMed: 12493558]

Moore TL, Killiany RJ, Herndon JG, Rosene DL, Moss MB, 2006 Executive system dysfunction occurs as early as middle-age in the rhesus monkey. Neurobiol. Aging 27 (10), 1484–1493. [PubMed: 16183172]

Moore TL, Bowley B, Shultz P, Calderazzo, Shobin E, Killiany RJ, Rosene DL, Moss MB, 2017 Chronic curcumin treatment improves spatial working memory but not recognition memory in middle-aged rhesus monkeys. Geroscience 39 (5–6), 571–584. [PubMed: 29047012]

Moore TL, Bowley BGE, Shultz PL, Calderazzo SM, Shobin EJ, Uprety AR, Rosene DL, Moss MB, 2018 Oral curcumin supplementation improves fine motor function in the middle-aged rhesus monkey. Somatosens. Mot. Res 35 (1), 1–10. [PubMed: 29447046]

Nam SM, Choi JH, Yoo DY, Kim W, Jung HY, Kim JW, Hwang IK, 2014 Effects of curcumin (Curcuma Longa) on learning and spatial memory as well as cell proliferation and neuroblast

differentiation in adult and aged mice by upregulating brain-derived neurotrophic factor and CREB signaling. J. Med. Food 17 (6), 641–649. [PubMed: 24712702]

Neumann H, Kotter MR, Franklin RJ, 2009 Debris clearance by microglia: an essential link between degeneration and regeneration. Brain 132 (February (Pt. 2)), 288–295. 10.1093/brain/awn109. [PubMed: 18567623]

Ng TP, Chiam PC, Lee T, et al., 2006 Curry consumption and cognitive function in the elderly. Am. J. Epidemiol 164 (9), 898–906. [PubMed: 16870699]

Noorafshan A, Karimi F, Karbalay-Doust S, Kamali AM, 2017 Using curcumin to prevent structural and behavioral changes of medial prefrontal cortex induced by sleep deprivation in rats. EXCLI J 16, 510–520. [PubMed: 28694754]

Olivera A, Moore TW, Hu F, Brown AP, Sun A, Liotta DC, Snyder JP, Yoon Y, Shim H, Marcus AI, Miller AH, Pace TW, 2012 Inhibition of the NF-κB signaling pathway by the curcumin analog, 3,5-Bis(2-pyridinylmethylidene)-4-piper-idone (EF31): anti-inflammatory and anti-cancer properties. Int. Immunopharmacol 12 (2), 368–377. [PubMed: 22197802]

Peters A, Kemper T, 2012 A review of the structural alterations in the cerebral hemispheres of the aging rhesus monkey. Neurobiol. Aging 33 (10), 2357–2372. [PubMed: 22192242]

Peters A, Sethares C, 2002 Aging and the myelinated fibers in prefrontal cortex and corpus callosum of the monkey. J. Comp. Neurol 442 (3), 277–291. [PubMed: 11774342]

Salat DH, Lee SY, van der Kouwe AJ, Greve DN, Fischl B, Rosas HD, 2009 Ageassociated alterations in cortical gray and white matter signal intensity and gray to white matter contrast. NeuroImage 48 (1), 21–28. [PubMed: 19580876]

Shobin E, Bowley MP, Estrada LI, Heyworth NC, Orczykowski ME, Eldridge SA, et al., 2017 Microglia activation and phagocytosis: relationship with aging and cognitive impairment in the rhesus monkey. GeroScience 39 (2), 199–220. [PubMed: 28238188]

Siddiqui AM, Cui X, Wu R, et al., 2006 The anti-inflammatory effect of curcumin in an experimental model of sepsis is mediated by up-regulation of peroxisome proliferator-activated receptor-γ. Crit. Care Med 34 (7), 1874–1882. [PubMed: 16715036]

Singh K, Trivedi R, Devi MM, Tripathi RP, Khushu S, 2016 Longitudinal changes in the DTI measures, anti-GFAP expression and levels of serum inflammatory cytokines following mild traumatic brain injury. Exp. Neurol 275, 427–435. [PubMed: 26216663]

Sloane JA, Hollander W, Moss MB, et al., 1999 Increased microglial activation and protein nitration in white matter of the aging monkey. Neurobiol. Aging 20 (4), 395–405. [PubMed: 10604432]

Smith RS, Koles ZJ, 1970 Myelinated nerve fibers: computed effect of myelin thickness on conduction velocity. Am. J. Physiol 219 (5), 1256–1258. [PubMed: 5473105]

Tomimoto H, Akiguchi I, Wakita H, Lin JX, Budka H, 2000 Cyclooxygenase-2 is induced in microglia during chronic cerebral ischemia in humans. Acta Neuropathol. Acta Neuropathol 99 (January (1)), 26–30. [PubMed: 10651024]

von Bernhardi R, Eugenín-von Bernhardi L, Eugenín J, 2015 Microglial cell dysregulation in brain aging and neurodegeneration. Front. Aging Neurosci 20 (July (7)), 124 10.3389/fnagi.2015.00124.

Wang SH, Morris RGM, 2010 Hippocampal-neocortical interactions in memory formation, consolidation, and reconsolidation. Annu. Rev. Psychol 61 49–79 C1–4. [PubMed: 19575620]

Wedeen VJ, Wang RP, Schmahmann JD, Benner T, Tseng WYI, Dai G, Pandya DN, Hagmann P, D'Arceuil H, de Crespigny AJ, 2008 Diffusion spectrum magnetic resonance imaging (DSI) tractogra-phy of crossing fibers. NeuroImage 41, 1267–1277. [PubMed: 18495497]

Wisco JJ, Killiany RJ, Guttmann CR, Warfield SK, Moss MB, Rosene DL, 2008 An MRI study of age-related white and gray matter volume changes in the rhesus monkey. Neurobiol. Aging 29 (10), 1563–1575. [PubMed: 17459528]

Xie F, Zhang JC, Fu H, Chen J, 2013 Age-related decline of myelin proteins is highly correlated with activation of astrocytes and microglia in the rat CNS. Int. J. Mol. Med 32 (5), 1021–1028. [PubMed: 24026164]

Yeh FC, Wedeen VJ, Tseng WY, 2010 Generalized q-sampling imaging. IEEE Trans. Med. Imaging 29 (9), 1626–1635. [PubMed: 20304721]

Yeh FC, Liu L, Hitchens TK, Wu YL, 2016 Mapping immune cell infiltration using restricted diffusion MRI. Magn. Reson. Med 77 (2), 603–612. [PubMed: 26843524]

Yu S, Wang X, He X, et al., 2016 Curcumin exerts anti-inflammatory and anti-oxidative properties in 1-methyl-4-phenylpyridinium ion (MPP++)-stimulated mesencephalic astrocytes by interference with TLR4 and downstream signaling pathway. Cell Stress Chaperones 21 (4), 697–705. 10.1007/s12192-016-0695-3. [PubMed: 27164829]

Yuan J, Liu W, Zhu H, Chen Y, Zhang X, Li L, et al., 2017 Curcumin inhibits glial scar formation by suppressing astrocyte-induced inflammation and fibrosis in vitro and in vivo. Brain Res 1655, 90–103. [PubMed: 27865778]

Zhang Y, Brady M, Smith S, 2001 Segmentation of brain MR images through a hidden Markov random field model and the expectation maximization algorithm. IEEE Trans. Med. Imaging 20 (1), 45–57. [PubMed: 11293691]

Zhang L, Xu T, Wang S, Yu L, Liu D, Zhan R, Yu SY, 2012 Curcumin produces antidepressant effects via activating MAPK/ERK-dependent brain-derived neurotrophic factor expression in the amygdala of mice. Behav. Brain Res 235 (1), 67–72. [PubMed: 22820234]

Zheng K, Dai X, Xiao N, Wu X, Wei Z, Fang W, et al., 2017 Curcumin ameliorates memory decline via inhibiting BACE1 expression and β-amyloid pathology in 5×FAD transgenic mice. Mol. Neurobiol 54 (3), 1967–1977. [PubMed: 26910813]

Zhuo J, Xu S, Proctor JL, Mullins RJ, Simon JZ, Fiskum G, Gullapalli RP, 2012 Diffusion kurtosis as an in vivo imaging marker for reactive astrogliosis in traumatic brain injury. NeuroImage 59 (1), 467–477. [PubMed: 21835250]

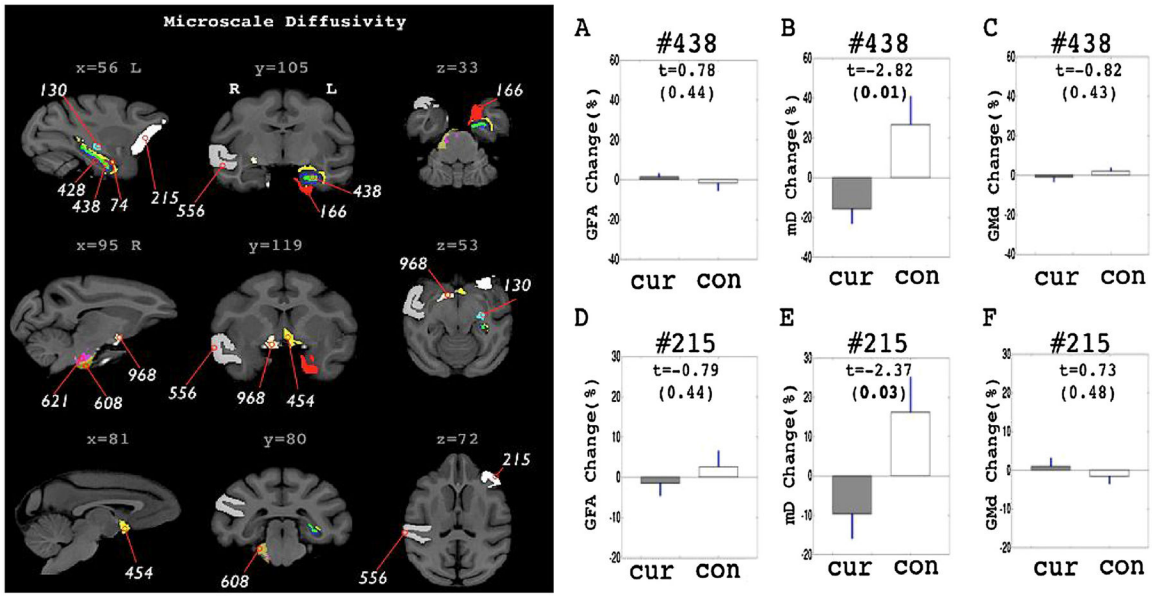


**Fig. 1.**

ROIs with significant group differences in the percent change pattern of microscale diffusivity (mD). ROIs are highlighted in the left panel with different color codings. ROI labels are identical to the one listed in the Table 2. GFA, mD and GMd change pattern in the hippocampal ROI (#438) is shown in A–C. GFA, mD and GMd change pattern in the prefrontal ROI (#215) is shown in D–F. ‘Cur’ in the graphs indicates curcumin treated group. ‘con’ indicates control group. In the graphs (A–F), Bar graph shows mean value of the percent change and blue line shows the standard error of mean. T stats and the significance levels are also marked inside the graph. Bold text indicates corrected $P < 0.05$ significance level.

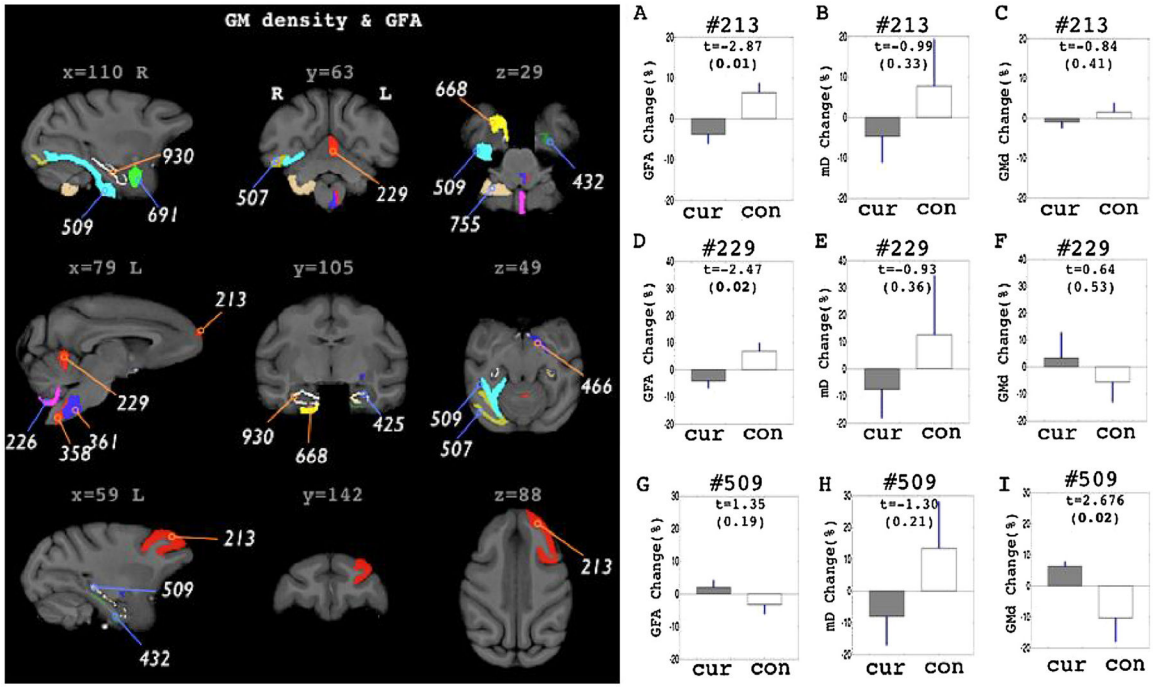


**Fig. 2.**

ROIs with significant group differences in the percent change pattern of GMd and GFA. ROIs are highlighted in the left panel with different color codings. ROIs selected in GFA assessments are shown in blue indication lines with ROI label. ROIs selected in GMd assessments are shown in orange indication lines with ROI label. Right panels shows 3 different measurements (GFA, mD, GMd) in the ROIs, #213 (A–C), #229 (D–F) and #509 (G–I). ‘Cur’ in the graphs indicates curcumin treated group. ‘con’ indicates control group. In the graphs (A–F), Bar graph shows mean value of the percent change and blue line shows the standard error of mean (S.E.M). T stats and the significance levels are also marked inside the graph. Bold text indicates corrected $P < 0.05$ significance level.

**Table 1**

Demographic information and cognitive assessments on 16 rhesus monkeys used for the imaging analyses. One female monkey in the curcumin group was excluded for the analysis due to the reconstruction error on the follow up scan. Cognitive measures shows mean value and the standard error of mean of each group. Percentage improvement in round 2 measurements were calculated as follows: (Round2 − Round1)/Round1 * 100.

| | age | Gender (M/F) | DNMS1st | DNMS2nd | DNMS improve (%) | DRSTsp1 | DRST2nd | DRST improve (%) |
|---|---|---|---|---|---|---|---|---|
| Curcumin | 15.83 (2.89) | 4/6 | 82.5 (0.78) | 80.0 (0.65) | 2 (1.1) | 1.98 (0.02) | 2.42 (0.04) | 22.4 (1.59) |
| Control | 13.88 (2.46) | 2/4 | 79.2 (0.55) | 83.17 (1.53) | 5 (1.8) | 2.35 (0.13) | 2.49 (0.06) | 11.7 (4.5) |

**Table 2**

ROIs with significant group differences in the percent change pattern of mD, GMd and GFA. ROI labels are randomized numbers. Anatomical labels are shown in the ROI section. The percent change pattern of mD, GFA and GMd in each group is shown in the 'FollowUp-Baseline % change section. Mean and S.E.M is shown in each ROIs. 'T' shows t statistics. '**' mark indicates corrected $p < 0.02$ significance level. Other ROIs without '**' mark are in corrected $p < 0.05$.

| index | ROI label | ROI | FollowUp-Baseline ± % change Curcumin | Control | T |
|---|---|---|---|---|---|
| mD | | *Hippocampal and near ROIs* | | | |
| | #438 | l_hilus_of_the_dentate_gyrus | −15.81 ± 7.69 | 26.35 ± 14.64 | −2.82** |
| | #428 | l_molecular_layer_of_the_dentate_gyrus | −16.55 ± 9.74 | 27.59 ± 17.59 | −2.39 |
| | #74 | l_temporal_horn_of_the_lateral_ventricle | −12.27 ± 7.58 | 20.44 ± 13.99 | −2.26 |
| | #166 | l_entorhinal_area | −20.90 ± 10.40 | 34.83 ± 21.22 | −2.65 |
| | | *Other subcortical ROIs* | | | |
| | #454 | l_nucleus_of_the_diagonal_band | −15.72 ± 8.46 | 26.21 ± 12.51 | −2.87** |
| | #968 | r_basal_forebrain_nucleus | −15.24 ± 9.07 | 25.40 ± 10.56 | −2.84** |
| | #130 | l_lateral_geniculate_nucleus | −16.79 ± 8.21 | 27.99 ± 15.24 | −2.84** |
| | | *Pons/CST ROIs* | | | |
| | #608 | r_middle_cerebellar_peduncle | −18.38 ± 7.94 | 30.64 ± 24.51 | −2.31 |
| | #621 | r_pontine_nuclei | −13.66 ± 7.89 | 22.77 ± 12.89 | −2.56 |
| | | *Cortical ROIs* | | | |
| | #215 | l_fronto-orbital_gyrus | −9.67 ± 6.45 | 16.11 ± 9.07 | −2.37 |
| | #556 | r_superior_temporal_gyrus | −10.50 ± 7.79 | 17.50 ± 10.39 | −2.18 |
| GFA | | *Hippocampal and near ROIs* | | | |
| | #930 | r_molecular_layer_of_the_dentate_gyrus | 4.34 ± 2.93 | −7.31 ± 3.96 | 2.41 |
| | #668 | r_entorhinal_area | −4.54 ± 2.61 | 7.56 ± 5.45 | −2.26 |
| | | Other subcortical ROIs | | | |
| | #466 | l_basal_forebrain_nucleus | 4.93 ± 3.01 | −8.22 ± 4.32 | 2.57 |
| | | *Pons/CST ROIs* | | | |
| | #358 | l_intermediate_reticular_nucleus | 7.86 ± 6.65 | −13.11 ± 3.30 | 2.32 |
| | #361 | l_gigantocellular_nucleus | 5.61 ± 3.38 | −9.35 ± 6.21 | 2.32 |
| | | *Cerebellar ROIs* | | | |
| | #229 | l_lobule_IV | −4.08 ± 2.76 | 6.8 ± 3.34 | −2.46 |

| index | ROI label | ROI | FollowUp-Baseline ± % change Curcumin | Control | T |
|---|---|---|---|---|---|
| | | *Cortical ROIs* | | | |
| | #213 | l_middle_frontal_gyrus | −3.85 ± 2.35 | 6.42 ± 2.41 | −2.87** |
| | Gmd | *Hippocampal and near ROIs* | | | |
| | #425 | l_granular_layer_of_the_dentate_gyrus | −12.19 ± 7.79 | 20.31 ± 11.57 | −2.42 |
| | #166 | l_entorhinal_area | −3.78 ± 2.92 | 6.29 ± 2.81 | −2.3 |
| | #432 | l_subiculum | −7.43 ± 4.37 | 12.39 ± 6.49 | −2.62 |
| | | *Other subcortical ROIs* | | | |
| | #691 | r_lateral_amygdalar_nucleus | −4.65 ± 3.01 | 7.75 ± 2.66 | −2.79** |
| | | *Cerebellar ROIs* | | | |
| | #226 | l_uvula | −12.08 ± 3.99 | 20.13 ± 15.82 | −2.46 |
| | #755 | r_biventer_lobule | −9.89 ± 1.81 | 16.49 ± 11.15 | −3.02** |
| | | *Cortical ROIs* | | | |
| | #509 | r_fusiform_gyrus | 6.26 ± 1.71 | −10.44 ± 7.71 | 2.68 |
| | #507 | r_inferior_occipital_gyrus | 5.03 ± 2.58 | −8.39 ± 6.69 | 2.2 |